CrystEngComm

www.rsc.org/crystengcomm

Volume 11 | Number 11 | November 2009 | Pages 2213–2554

RSC Publishing

COVER ARTICLE
Yu *et al.*
Facile synthesis and shape evolution of highly symmetric 26-facet polyhedral microcrystals of Cu_2O

HIGHLIGHT
Dance and Scudder
Molecules embracing in crystals

HOT ARTICLE
Shi *et al.*
Growth and characterization of ZnS porous nanoribbon array constructed by connected nanocrystallites

Facile synthesis and shape evolution of highly symmetric 26-facet polyhedral microcrystals of Cu_2O†

Weiwei Zhou, Bin Yan, Chuanwei Cheng, Chunxiao Cong, Hailong Hu, Hongjin Fan and Ting Yu*

Received 18th June 2009, Accepted 30th July 2009
First published as an Advance Article on the web 18th August 2009
DOI: 10.1039/b912034n

A novel type of high symmetric 26-facet polyhedral microcrystals of Cu_2O with well-developed {100}, {110}, {111} crystallographic faces are successfully synthesized in a properly selected reaction medium. These polyhedra exhibit a core-shell structure. An aqueous solution containing $CuCl_2 \cdot 2H_2O$, sodium citrate ($C_6H_5Na_3O_7 \cdot 2H_2O$) complexing agent, glucose reductant, sodium dodecyl sulfate (SDS) surfactant, NaOH, and ethylene glycol (EG) constitutes the functional medium. By altering the EG to the water volume ratio, polyhedral, quasi-cubic, octahedral microcrystals are obtained directly. SDS, EG and $C_6H_5Na_3O_7 \cdot 2H_2O$ have been confirmed to be the necessary additives to the development of different crystallographic planes. A possible growth mechanism involving aggregation of seed particles, oriented attachment, ripening process and surface reconstruction is proposed on the grounds of time-dependent experiments. The photocatalytic properties of the polyhedral microcrystals are also investigated.

1. Introduction

In the research of mesoscopic material sciences, developing methods for tailoring of the materials' morphologies has been one of the important topics,[1–3] as these materials generally exhibit many size- and shape- dependent properties which are interesting for device applications.[4–6] In particular, shape-controlled synthesis of metal oxide semiconductors in the nano/micro dimensions is essential not only for better understanding and manipulation of the kinetics of the crystal growth, but also for the exploration of their novel applications.[7] Cuprous oxide (Cu_2O), as a small (~2 eV) direct bandgap p-type semiconductor, has attracted great attention due to its wide range of applications in solar energy conversion,[3,8] photocatalytic degradation of organic pollutants,[9,10] photoactivated splitting of water into O_2 and H_2 under visible light,[11,12] and in lithium ion batteries.[13,14] Cu_2O is also a paradigm material for research on the Bose–Einstein condensation.[15] Moreover, Cu_2O is non-toxic, inexpensive and abundant in nature. To date, numerous Cu_2O nano/micro crystals such as one-dimensional nanostructures (nanowires, nanorods and nanotubes),[16–18] cubes,[8,19,20] octahedra,[21,22] cages,[23,24] multipod microcrystals,[25] nanospheres or hollow spheres,[26,27] and some three-dimensional architectures (hexpod-like whiskers, stellar, star-like and flower-like crystals)[28–30] have been prepared.

Although various methods including thermal oxidation, chemical vapor deposition, electrochemical synthesis and emulsion reduction have been employed to synthesize Cu_2O nanocrystals,[31–34] most of these existing techniques require complex reaction conditions. Moreover, a precise-control synthesis and in-depth understanding of the morphology evolution of those unconventional microscopic structures of Cu_2O are still challenging. Therefore, strategies for low-cost, low-temperature and simple synthesis of Cu_2O are highly desirable.

In this study, we have developed a facile hydrothermal procedure for the synthesis of Cu_2O microcrystals with different morphologies by adopting a polyol process at low temperature. In addition to common quasi-cubic and octahedral microcrystals, we obtained, for the first time, a novel type of uniform 26-facet polyhedra with well-defined {100}, {110}, {111} faces under moderate conditions. Interestingly, these 26-facet Cu_2O polyhedra exhibit a core-shell structure. Our proper choice of reactants not only favors the formation of 26-facet polyhedral morphology, but also allows for the reaction to occur at low temperature (90 °C). Based on the results of time-dependent experiments, a possible crystal growth process is proposed, which involves the aggregation of seed particles, oriented attachment, and ripening process. In addition, the photodegradation ability of the products under a normal fluorescent lamp will be shown, which indicates the feasibility of their practical photocatalytic applications.

2. Experimental

2.1 Synthesis of 26-facet polyhedral microcrystals of Cu_2O

All chemicals were analytical grade and used without further purification. In a typical synthesis, two identical sets of solvents were prepared by mixing 15 mL EG and 5 mL deionized water. 0.5 mmol SDS was added to each set and stirred until the complete dissolution of SDS. Subsequently, 0.75 mmol $CuCl_2 \cdot 2H_2O$ and 0.5 mmol $C_6H_5Na_3O_7 \cdot 2H_2O$ were added to these two solutions, respectively. 10 min later, the $C_6H_5Na_3O_7 \cdot 2H_2O$ solution was poured into the $CuCl_2 \cdot 2H_2O$ solution, followed by the addition of 2 mmol

Division of Physics and Applied Physics, School of Physical and Mathematical Sciences, Nanyang Technological University, Singapore, 637371. E-mail: yuting@ntu.edu.sg; Tel: +65-6316-7899

† Electronic supplementary information (ESI) available: FESEM images of the samples obtained by changing the $C_6H_5Na_3O_7 \cdot 2H_2O$ with (a) NaCl; (b) Na_2SO_4; (c) $NaNO_3$ (Fig. S1); FESEM image of the sample obtained in the absence of SDS (Fig. S2). See DOI: 10.1039/b912034n

glucose and 10 mL 0.1 M aqueous NaOH. Another 10 min later, 40 mL of the resulting mixture was transferred into a 50 mL Teflon-lined stainless steel autoclave, sealed and maintained at 90 °C for 20 h. Magnetic stirring was continuously applied throughout the entire process before transferring to the autoclave. After the reaction was complete, the product was collected, washed several times with absolute ethanol and deionized water, centrifuged, and dried in the air at room temperature for 12 h.

2.2 Characterizations

The powder X-ray diffraction (XRD) analysis was performed using a D8 Advanced diffractometer with Cu Kα line. Transmission electron microscopy (TEM) images were recorded by a JEOL JEM-1400 F transmission electron microscope with an accelerating voltage of 200 kV. Field-emission scanning electron microscopy (FESEM) analysis was conducted with a JEOL JSM-6700F electron microscope. Room-temperature UV-vis absorption spectrum was recorded on a UV-2550 spectrophotometer in the wavelength range of 250–650 nm.

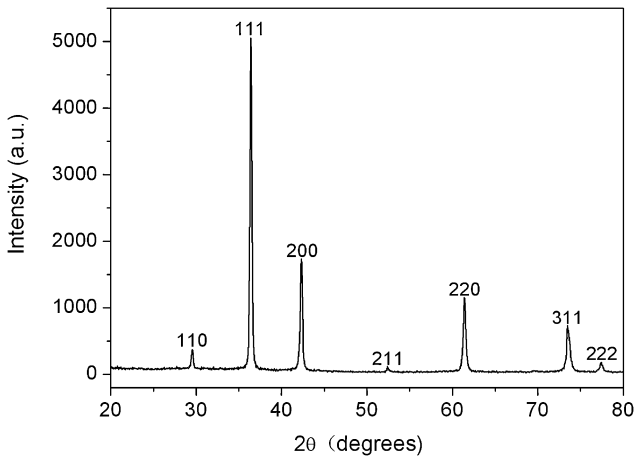

Fig. 1 XRD pattern of the synthesized 26-facet polyhedral microcrystals of Cu_2O.

3. Results and discussion

3.1 Microstructure examination

Fig. 1 shows an X-ray diffraction (XRD) spectrum of the as-prepared Cu_2O polyhedral microcrystals with 26 faces. All peaks are clearly distinguishable and can be perfectly indexed to the cubic phase Cu_2O (JCPDF 005–0667) in terms of the peak positions and their relative intensities. The peaks with 2θ values of 29.5, 36.4, 42.3, 61.3, and 73.4° correspond to the crystal planes of (110), (111), (200), (220), and (311) of the crystalline Cu_2O, respectively. No other diffraction peaks appear in the XRD pattern, implying the absence of impurities such as metallic copper or cupric oxide.

The morphologies of the as-synthesized polyhedral Cu_2O microcrystals were investigated by FESEM and TEM. A typical low magnification SEM image clearly indicates that the product is almost composed of uniform polyhedra with an overall size of 3–4 μm (Fig. 2a). These microstructures can be clearly identified to be a 26-facet polyhedral morphology with all well-developed faces and edges (Fig. 2b). Some of the polyhedra are broken on the surfaces revealing their core-shell structure with a spherical core (Fig. 2c). The TEM image in Fig. 2d also shows the polyhedral outline (the lack of contrast is because the crystal is too thick for the electrons to penetrate). A schematic model is provided for a clear illustration of the 26-facet morphology of the microcrystal (Fig. 2e). It can be seen that each 26-facet polyhedron contains six square {100} faces, twelve rectangular {110} faces and eight triangular {111} faces. Therefore, it is an Archimedean-type polyhedron (*i.e.*, all vertices are identical). This structure can also be viewed as a cube with truncated corners and edges. Also, as the polyhedron has 26 facets, 24 vertices and 48 edges, it satisfies Euler's equation,[35] which correlates the number of polyhedron vertices V, faces F and edges E as:

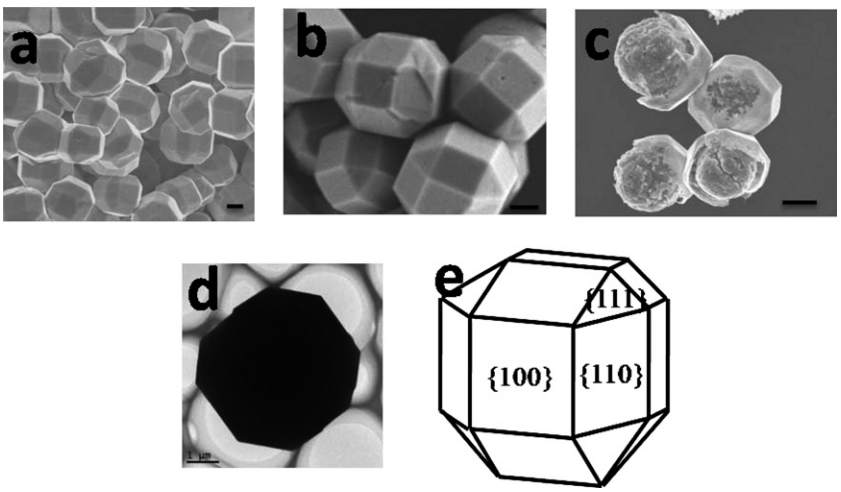

Fig. 2 (a)–(c) FESEM images of 26-facet Cu_2O polyhedra; (d) TEM image of 26-facet Cu_2O polyhedron. (e) schematic model of 26 - facet Cu_2O polyhedral. The scale bar is 1 μm.

$$V + F - E = 2$$

According to Gibbs–Wulff's theorem[36]

$$\frac{\gamma_1}{h_1} = \frac{\gamma_2}{h_2} = \frac{\gamma_3}{h_3} = \cdots = \text{constant}$$

Where γ_n is the surface tension of the crystal face n, and h_n is the distance of that face from the Wulff's point in the crystal. Therefore, as for cubic phase, a relationship of $\gamma_{\{111\}} < \gamma_{\{100\}} < \gamma_{\{110\}}$ can be straightforwardly deduced based on the difference in the distances from these three faces to the central Wulff's point. Faces with a higher surface energy will eventually suffer elimination or reduction from the final appearance. It is known that, under equilibrium conditions, the crystal habit of inorganic crystals is determined by the relative order of surface energies.[37] The fastest growth occurs in the direction perpendicular to the faces with the highest surface energy. Therefore, a 26-facet polyhedron of cubic phase Cu_2O with co-presence of {100}, {110}, {111} faces will not form under equilibrium growth conditions without any additives. However, in a real reaction when additives are added, there exist some deviations from Wulff's theorem. Organic or inorganic additives added during the crystal growth can alter the relative order of surface energies when they selectively adsorb onto a certain crystallographic plane.[38] This preferential adsorption leads to lowering the surface energy of the bound plane and hinders the crystal growth perpendicular to this plane, resulting in a change in the final morphology. As a matter of fact, this has been a common approach to the modification of crystal morphology in materials science research.[23,39]

3.2 Effect of EG to water volume ratio

In the present study, EG–H_2O mixture with fixed volume ratio was used as solvent. In order to investigate the common effect of mixed solvents on the morphology development, a series of control experiments with different EG to water volume ratios were conducted. As the simplest polyol, EG is a popular industrial solvent and has been widely used as solvent and reducing agent in the so-called polyol synthesis of metals and semiconductor micro- and nanocrystals.[40–43] As shown in Fig. 3, when pure EG was adopted as the solvent, some microcrystals with quasi-cubic morphologies were obtained (Fig. 3a). Then, an addition of small amounts of water gave rise to the formation of uniform 26-facet polyhedra (Fig. 3b). Further increase of the water content resulted in a shape transformation from 26-facet polyhedra to octahedra (Fig. 3c and d). Finally, when pure water was used, the products were mainly irregular particles with a small number of octahedra (Fig. 3e).

As we know, higher water content induces faster ion transfer rate. Therefore, SDS, as a water-soluble amphiphile, would not exert a strong influence on the shape of the product under the conditions of low water content. Instead, EG was expected to be responsible for the quasi-cubic structure. It has been reported that EG could allow smaller irregular Cu_2O nanocrystals to assemble to nanoboxes (a type of cubic structure).[43] In our case, pure EG solvent also resulted in quasi-cubic Cu_2O microcrystals (see Fig. 3a). The deviation from perfect cubic is most likely due to the existence of a small amount of water coming from the aqueous NaOH solution, as well as possibly the rest of the additives. With increasing the fraction of water, the EG concentration became lower. Subsequently, the role of SDS for stabilizing the {111} planes of Cu_2O crystals began to dominate in the system, and an octahedral morphology formed due to the preferential adsorption of SDS onto {111} face to constrain the growth rates along the <111> direction.[44] The optimum volume ratio of EG to water in our system for the formation of 26-facet Cu2O polyhedra was found to be 75F : 25%. As mentioned above, the crystal growth habit is determined by the relative order of surface energies. Therefore, in this case, the co-presence of {111}, {100}, {110} faces indicates that the surface energies of these three faces (γ{111},γ{100},γ{110}) under the influence of additives, must be of the similar order so that they can appear at the same time. As can be seen from above, in our polyol-based growth, the function of EG is both solvent and a cubic structure-defining agent. It was not a reducing agent since the reaction only occurred at 90 °C.

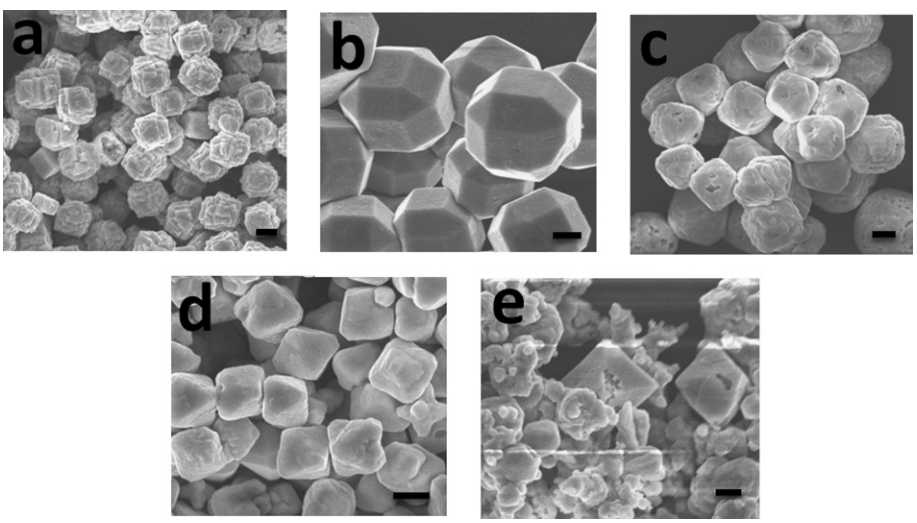

Fig. 3 FESEM images of Cu_2O microcrystals obtained at different volume ratios of EG to water: (a) 100:0%; (b) 75:25%; (c) 50:50%; (d) 25:75%; (e) 0:100%. The total volume is 40 mL. The scale bar is 1 μm.

3.3 Effect of $C_6H_5O_7^{3-}$ anions

In order to indentify the influence of $C_6H_5O_7^{3-}$ anions, control experiments were carried out with different sodium salts. Here, we selected sodium sulfate (Na_2SO_4), sodium chloride (NaCl) and sodium nitrate ($NaNO_3$). When SO_4^{2-} and Cl^- ions were adopted, blue precipitates emerged immediately after the addition of aqueous NaOH; no red Cu_2O appeared even after dwelling at 90 °C for 20 h. In the case of NO^{3-} ions, an addition of NaOH also generated blue precipitates but only after the mixture was kept at 90 °C for 20 h; still no red Cu_2O precipitates occurred (see Fig. S1).† These facts imply that the function of $C_6H_5O_7^{3-}$ anions in the present study is twofold: First, they are a complexing agent. The $C_6H_5O_7^{3-}$ anions was coordinated with Cu^{2+} to form complex $[Cu(C_6H_5O_7^{3-})_n]$, which prevented the formation of copper hydroxide in the initial mixture. Under a relatively higher reaction temperature (90 °C), the balance of the coordination between Cu^{2+} and $C_6H_5O_7^{3-}$ shifted and Cu^{2+} ions were gradually released, resulting in the formation of copper hydroxide. The copper hydroxide was then reduced to cuprous oxide. Second, the $C_6H_5O_7^{3-}$ anions also serve as a reducing agent (together with the glucose) as the presence of NO^{3-} anions does not result in red Cu_2O crystals.

A brief conclusion can be drawn now. The key factor to the development of such unconventional 26-facet polyhedra is an appropriate choice of reactants and a subtle combination of mixed solvents' volume ratio. Although the specific absorption ability of each additive is unclear, it is found that none of them is superfluous to the formation of 26-facet Cu_2O polyhedra. For EG, as can be seen from the above results, in addition to being the solvent, it was also an additive helping to stabilize {100} faces. Furthermore, its polarity and viscosity might have played a role in controlling the growth kinetics of Cu_2O microcrystals. Moreover, SDS is also proven to be indispensable for the formation of 26-facets Cu_2O polyhedral since only polyhedra with defective surfaces were obtained in the absence of SDS (Fig. S2).† As mentioned above, when several additives coexist in one medium, a lower strength between the additives and the bound plane will make the corresponding planes diminish or vanish, whereas the planes with a stronger link will survive. In our case, the strengths between the {111}, {100}, {110} planes and their corresponding additives might be of a similar level so as to ensure their co-presence. All in all, the observed 26-facet polyhedral morphology can be the result of a synergic effect of all three additives: $C_6H_5O_7^{3-}$ complexing anions, SDS surfactant, and EG.

3.4 Time-dependent experiments and growth mechanism

In order to shed light on the formation process of the Cu_2O polyhedral microcrystals, the shape evolution was examined by conducting synthesis of various reaction times. After 2 h of reaction, the products are mainly rough quasi-spherical particles with a few cubes (Fig. 4a). The aggregates of the small particles on the surface can be clearly seen. When the reaction time was increased to 5 h, an overall quasi-cubic shape is developed, although their surface is still rather rough (Fig. 4b). It is noteworthy that most of the quasi-cubes have already slightly truncated corners and edges. After a reaction time of 10 h, rudiments of polyhedra come into existence but still with some surface defects (Fig. 4c). When the reaction is prolonged to 15 h, the surface roughness decreases (Fig. 4d). After a reaction for 20 h, perfect 26-facet polyhedra with smooth surfaces and sharp edges are obtained (Fig. 4e).

Based on the above results, a possible growth mechanism is proposed as follows. At an initial stage, a large amount of small Cu_2O crystallites nucleate, grow into seed particles, and aggregate. The aggregation process continues, forming the observed quasi-spherical particles with an overall size of 2–3 μm (see Fig. 4a). Seed particles continuously attach onto these intermediate structures to allow further growth through a ripening process. In this stage, an oriented-attachment process dominates, while at the subsequent stage a ripening process dominates, resulting in the shape evolution from quasi-spherical to perfect 26-facet polyhedral *via* surface reconstruction. Therefore, a synergic effect of both ripening and oriented attachment processes accounts for the development of the final 26-facet Cu_2O polyhedra. The core-shell structure might also be due to the ripening process.

3.5 Photocatalytic characterization

To evaluate the photocatalytic activity of the Cu_2O microcrystals, photodegradation of methyl orange under visible

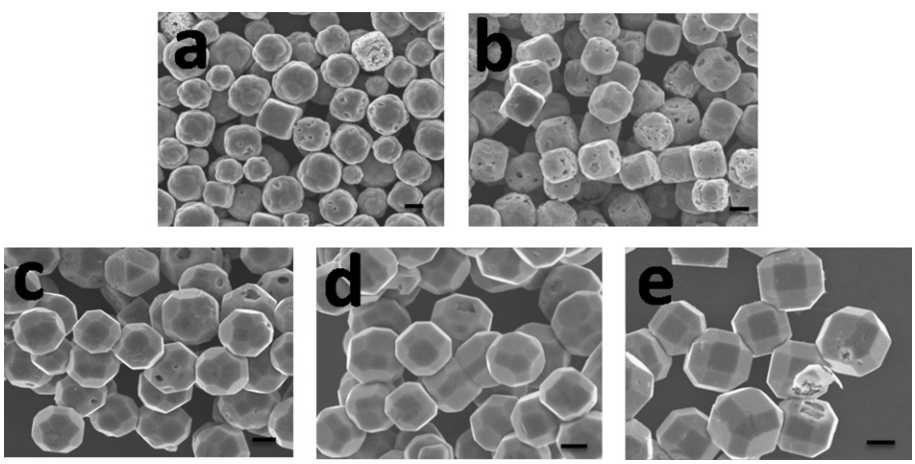

Fig. 4 FESEM images of Cu_2O microcrystals obtained at reaction times of (a) 2 h, (b) 5 h, (c) 10 h, (d) 15 h, (e) 20 h. The scale bar is 1 μm.

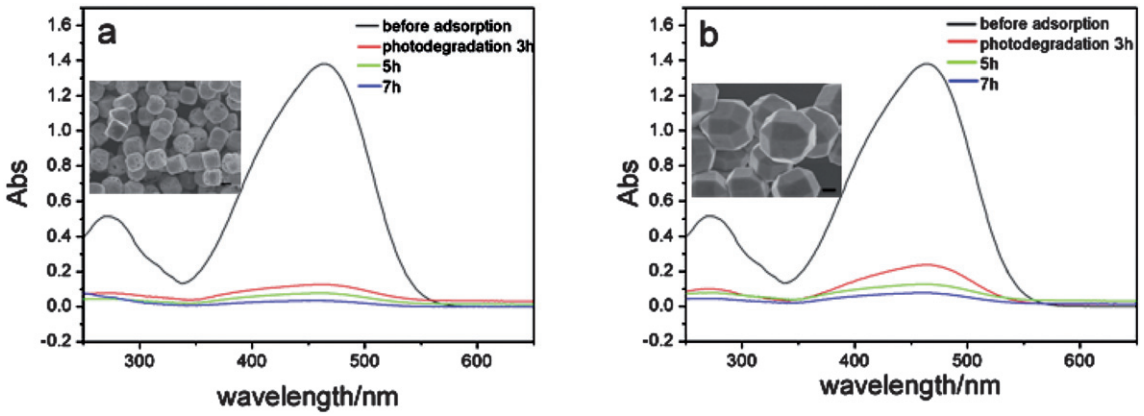

Fig. 5 Absorption spectrum of a solution of Methyl Orange in the presence of (a) quasi-cubic Cu_2O particles. (b) 26-facet polyhedral Cu_2O particles. The insets are their corresponding FESEM images. The scale bar is 1 μm.

light irradiation was selected as reference and the characteristic absorption of Methyl Orange at about 465 nm was selected for monitoring the photocatalytic degradation process. Here, we chose two representative morphologies for comparing: quasi-cube (formed after 5 h) and 26-facet polyhedron (formed after 20 h). In a typical experiment, 2 mg of Cu_2O microcrystals was dispersed in 10 mL of 20 mg L^{-1} aqueous methyl orange solution. Then 2 mL of this solution was transferred to a standard quartz cell. The cell was exposed to visible light irradiation from a 100 W fluorescent lamp placed 20 cm away. Fig. 5 shows the absorption spectra of an aqueous solution of Methyl Orange photodegraded by quasi-cubic Cu_2O particles (Fig. 5a) and 26-facet polyhedral Cu_2O particles (Fig. 5b) at different stages. As can be seen, the photocatalytic activity of the polyhedral Cu_2O particles is not higher than that of quasi-cubic particles, which is out of our expectation. The possible reasons are as follows: first, the quasi-cubic crystals are smaller in overall sizes than the 26-facet polyhedral (see Fig. 4 b and e) and the former has a porous surface. This means that the quasi-cubic crystals effectively have larger surface areas than the polyhedra. Second, it has been reported that {111} planes possess a higher activity than {100} planes.[10] Although the polyhedral microcrystals have six {111} faces among the 26 surface planes, the surface areas of the {111} faces are still too small to make an observable effect. Note that the photodegradation experiment of methyl orange here was carried out under the illumination by a normal fluorescent lamp. This indicates the potential application is quite feasible in practice.

4. Conclusion

We have reported a simple approach for the fabrication of highly symmetric 26-facet polyhedral microcrystals of Cu_2O by adopting a polyol process at low temperature. The basic reaction medium contains $CuCl_2 \cdot 2H_2O$, $C_6H_5Na_3O_7 \cdot 2H_2O$ complexing agent, glucose reductant, SDS surfactant, NaOH, and EG. Quite interestingly, these 26-facet polyhedra appear to possess a core-shell structure. It is found that the formation of such polyhedral microcrystals is strongly dependent on the presence of the above additives, the EG to water volume ratios, and the reaction time. Our Cu_2O microcrystals show good photocatalytic properties even under normal illumination by a fluorescent lamp, which indicates its practice application potentials.

References

1 Y. Xie, J. X. Huang, B. Li, Y. Liu and Y. T. Qian, *Adv. Mater.*, 2000, **12**, 1523.
2 J. T. Sampanthar and H. C. Zeng, *J. Am. Chem. Soc.*, 2002, **124**, 6668.
3 P. C. Ohara, J. R. Heath and W. M. Gelbart, *Angew. Chem., Int. Ed. Engl.*, 1997, **36**, 1078.
4 T. Yu, Y. W. Zhu, X. J. Xu, K. S. Yeong, Z. X. Shen, P. Chen, C. T. Lim, J. T. L. Thong and C. H. Sow, *Small*, 2006, **2**, 80.
5 T. Yu, Y. W. Zhu, X. J. Xu, Z. X. Shen, P. Chen, C. T. Lim, J. T. L. Thong and C. H. Sow, *Adv. Mater.*, 2005, **17**, 1595.
6 X. G. Peng, L. Manna and W. D. Yang, *Nature*, 2000, **404**, 59.
7 W. U. Huynh, J. J. Dittmer and A. P. Alivisatos, *Science*, 2002, **295**, 2425.
8 L. F. Gou and C. J. Murphy, *Nano Lett.*, 2003, **3**, 231.
9 W. Shi, K. Lim and X. J. Liu, *J. Appl. Phys.*, 1997, **81**, 2822.
10 H. L. Xu, W. Z. Wang and W. J. Zhu, *J. Phys. Chem. B*, 2006, **110**, 13829.
11 M. Hara, T. Kondo, M. Komoda, S. Ikeda, K. Shinohara, A. Tanaka, J. N. Kondo and K. Domen, *Chem. Commun.*, 1998, 357.
12 P. E. Jongh, D. Vanmaekelbergh and J. J. Kelly, *Chem. Commun.*, 1999, 1069.
13 P. Poizot, S. Laruelle, S. Grugeon, L. Dupont and J. M. Tarascon, *Nature*, 2000, **407**, 496.
14 C. M. McShane and K.-S. Choi, *J. Am. Chem. Soc.*, 2009, **131**, 2561.
15 D. Snoke, *Science*, 1996, **273**, 1351.
16 W. Z. Wang, G. H. Wang, X. S. Wang, Y. J. Zhan, Y. K. Liu and C. L. Zheng, *Adv. Mater.*, 2002, **14**, 67.
17 Y. W. Tan, X. Y. Xue, Q. Peng, H. Zhao, T. H. Wang and Y. D. Li, *Nano Lett.*, 2007, **7**, 3723.
18 L. Liao, B. Yan, Y. F. Hao, G. Z. Xing, J. P. Liu, B. C. Zhao, Z. X. Shen, T. Wu, L. Wang, J. T. L. Thong, C. M. Li, W. Huang and T. Yu, *Appl. Phys. Lett.*, 2009, **94**, 113106.
19 J. C. Park, J. Kim, H. Kwon and H. Song, *Adv. Mater.*, 2009, **21**, 803.
20 C.-H. Kuo, C.-H. Chen and M. H. Huang, *Adv. Funct. Mater.*, 2007, **17**, 3773.
21 C. H. Lu, L. M. Qi, J. H. Yang, X. Y. Wang, D. Y. Zhang, J. L. Xie and J. L. Ma, *Adv. Mater.*, 2005, **17**, 2562.
22 M. J. Siegfried and K.-S. Choi, *Adv. Mater.*, 2004, **16**, 1743.
23 J. J. Teo, Y. Chang and H. C. Zeng, *Langmuir*, 2006, **22**, 7369.
24 C.-H. Kuo, C.-H. Chen and M. H. Huang, *J. Am. Chem. Soc.*, 2008, **130**, 12815.
25 Y. Chang and H. C. Zeng, *Cryst. Growth Des.*, 2004, **4**, 273.

26 H. Li, R. Liu, R. Zhao, Y. Zheng, W. Chen and Z. Xu, *Cryst. Growth Des.*, 2006, **6**, 2795.
27 J. T. Zhang, J. F. Liu, Q. Peng, X. Wang and Y. D. Li, *Chem. Mater.*, 2006, **18**, 867.
28 Z. Z. Chen, E. W. Shi, Y. Q. Zheng, W. J. Li, B. Xiao and J. Y. Zhuang, *J. Cryst. Growth*, 2003, **249**, 294.
29 Z. C. Wu, M. W. Shao, W. Zhang and Y. B. Ni, *J. Cryst. Growth*, 2004, **260**, 490.
30 Z. H. Liang and Y. J. Zhu, *Mater. Lett.*, 2005, **59**, 2423.
31 J. Tanori and M. P. Pileni, *Adv. Mater.*, 1995, **7**, 862.
32 D. W. Zhang, C. H. Chen, J. Zhang and F. Ren, *Chem. Mater.*, 2005, **17**, 5242.
33 Q. Y. Lu, F. Gao and D. Y. Zhao, *Nano Lett.*, 2002, **2**, 725.
34 H. P. Hentze, S. R. Raghavan, C. A. McKelvey and E. W. Kaler, *Langmuir*, 2003, **19**, 1069.
35 H. S. M. Coxeter, *Regular Polytopes*; New York: Dover, 1973, pp 9–11 and 165–172.
36 G. Wulff, *Z. Kristallogr.*, 1901, **34**, 449.
37 J. W. Mullin, *Crystallization*. Butterworths, London 1971.
38 H. E. Buckley, *Crystal Growth*, Wiley, New York 1951.
39 M. J. Siegfried and K.-S. Choi, *Angew. Chem., Int. Ed.*, 2005, **44**, 3218.
40 C. O. Zorica, A. Alojz, D. Goran and Z. Majda, *Cryst. Growth Des.*, 2007, **7**, 453.
41 J. Chen, T. Herricks, M. Geissler and Y. N. Xia, *J. Am. Chem. Soc.*, 2004, **126**, 10854.
42 Y. G. Sun and Y. N. Xia, *Adv. Mater.*, 2002, **14**, 833.
43 Y. Zhao, Y. Zhang, H. Zhu, G. C. Hadjipanayis and J. Q. Xiao, *J. Am. Chem. Soc.*, 2004, **126**, 6874.
44 L. Huang, F. Peng, H. Yu and H. J. Wang, *Mater. Res. Bull.*, 2008, **43**, 3047.

